

000 001 002 003 004 005 006 007 008 009 010 011 012 013 014 015 016 017 018 019 020 021 022 023 024 025 026 027 028 029 030 031 032 033 034 035 036 037 038 039 040 041 042 043 044 045 046 047 048 049 050 051 052 053 DATA DIVERSITY FOR COMPOSITIONAL GENERALIZATION

Anonymous authors

Paper under double-blind review

ABSTRACT

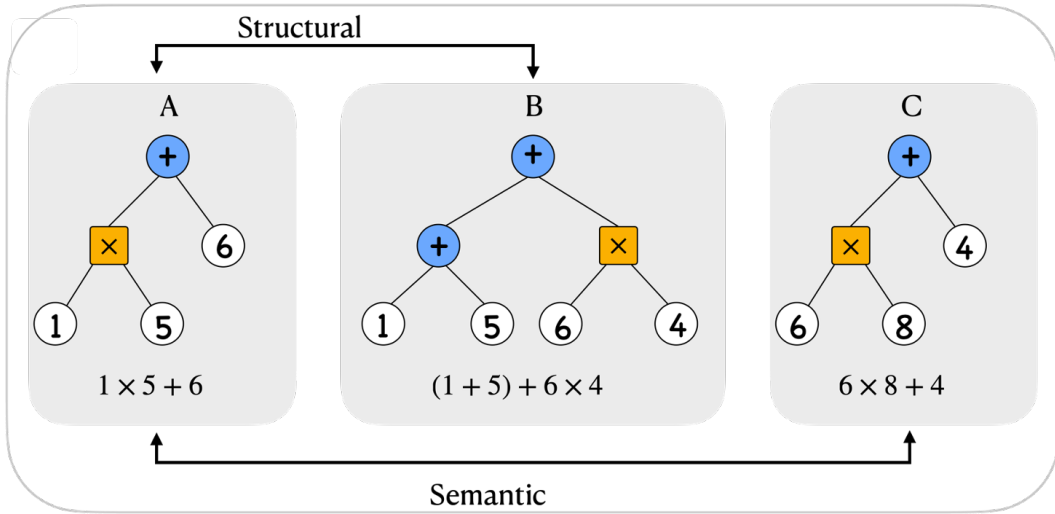
Human cognition excels at understanding complex concepts by composing simpler learned elements, enabling efficient learning and generalization to novel scenarios. Recent studies suggest that machine learning models may exhibit similar compositional capabilities by first acquiring fundamental components and then recombining them. A key driver of this process is the training data, and in particular, the statistical diversity of that data plays a crucial role in shaping a model’s ability to generalize. In this work, we introduce a framework that disentangles the multifaceted notion of diversity and formalize its impact on model performance and generalization ability from different perspectives. Through both theoretical analysis and empirical validation, we demonstrate that simply increasing data diversity without a principled strategy does not necessarily lead to improved generalization. Instead, achieving optimal generalization requires a principled understanding of data diversity. Guided by this insight, we propose a high-level set of guidelines for constructing and curating training datasets that facilitate more efficient learning and better generalization to unseen compositions.

1 INTRODUCTION

In recent years, artificial intelligence (AI) has achieved remarkable progress across a broad range of tasks, including language understanding and generation (Hurst et al., 2024; Liu et al., 2024; Grattafiori et al., 2024), reasoning and planning (Guo et al., 2025; Jaech et al., 2024), image and video generation (Dhariwal & Nichol, 2021; Wang et al., 2025), to name only a few. A major driver of this success is the unprecedented scale of training data (Kaplan et al., 2020). Modern AI systems are trained on data volumes that far exceed human experience, by some estimates, more than 200 lifetimes’ worth (Griffiths, 2020). As the scale of training data continues to grow and we are approaching practical and economic limits on collecting even more data for training (Villalobos et al., 2022; Muennighoff et al., 2023), improving data efficiency has become increasingly important. While substantial effort has devoted to improving data quality and developing data selection strategies (Xia et al., 2024; Albalak et al., 2024; Xie et al., 2023; Gu et al., 2024), an increasing number of studies are recognizing the importance of data diversity during training (Zhao et al., 2024; Miranda et al., 2023). However, diversity is a multifaceted concept, it encompasses variations in semantics, structures, and other properties. These different aspects can contribute differently to the model’s learning process. Developing a principled understanding of these aspects and their roles is a key step toward building AI systems that are more data efficient.

Motivated by these challenges, we study data diversity through the lens of compositionality, which is described as “*infinite use of finite means*” (Chomsky, 2014), examining its impacts on model generalization. Specifically, we examine how different forms of diversity impact a model’s ability to generalize compositionally; that is, to generalize to novel scenarios, by systematically recombining previously learned components and rules, which is referred to as compositional generalization. This capability is a hallmark of human cognition (Frankland & Greene, 2020; Dehaene et al., 2022; Elmoznino et al., 2024) and equally influential and important in AI, inspiring diverse research directions, including neuro-symbolic model (Soulos et al., 2023; 2024), disentangled representation learning (Wang et al., 2024b; Higgins et al., 2017), chain-of-thought reasoning (Wei et al., 2022), and some prompt engineering methods (Drozdov et al., 2022). A key advantage of compositional generalizing ability is that once a model learns to represent and manipulate the features in training data compositionally, it can generalize to novel combinations of those features without having

054 encountered them during training (Lake & Baroni, 2018; Mittal et al., 2021). This property is cru-
 055 cial for data-efficient learning (Wiedemer et al., 2023), enabling models to leverage a limited set of
 056 examples to generalize across a much larger combinatorial space.
 057



058
 059
 060
 061
 062
 063
 064
 065
 066
 067
 068
 069
 070
 071
 072
 073
 074
 075 Figure 1: Example of semantic and structural diversity. In this algebraic circuit, A-B illustrates
 076 structural diversity: different circuit structures representing distinct compositional forms. In
 077 contrast, A-C illustrates semantic diversity: multiple surface realizations (different input values)
 078 that share the same underlying structure. The number of such realizations per structure reflects its degree
 079 of semantic diversity.
 080

081 Training data plays a distinct role in enabling compositional generalization, since compositionality is
 082 a property of the data-generating process (Wiedemer et al., 2023; Zimmermann et al., 2021). Learning
 083 can be viewed as the inverse of this process, where the model infers underlying compositional
 084 components and then recombines these components to generalize beyond them. Prior work (Park
 085 et al., 2024; Okawa et al., 2023; Wiedemer et al., 2023) identifies two essential steps in achiev-
 086 ing compositional generalization: (1) acquiring the fundamental conceptual components, and (2)
 087 systematically recombining them to generalize to novel compositions.
 088

089 In this work, we study how data diversity, and its different aspects, support these processes under a
 090 constrained data budget. [While prior work has explored the role of data diversity in compositional](#)
 091 [ability \(Akyürek & Andreas, 2022; Zhou et al., 2023; Uselis et al., 2025\)](#), we formalize data diver-
 092 sity along two different dimensions: *semantic diversity*, which refers to varied surface realizations
 093 of the same underlying structure, and *structural diversity*, which captures a broader range of dis-
 094 tinct compositional structures. Building on this distinction, we develop a theoretical framework to
 095 analyze how semantic and structural diversity contribute to models’ compositional generalization
 096 ability under limited data. Our framework provides high-level guidelines for balancing these two di-
 097 mensions of data diversity under a constrained data budget to maximize generalization. To validate
 098 our framework, we conduct controlled experiments on synthetic datasets of algebraic circuits (Wang
 099 et al., 2024a; Ito et al., 2024; Savage, 1998), which naturally supports decomposition and recombi-
 100 nation of compositional structures. We then investigate how the theoretical insights and the controlled
 101 setting can be extended to realistic scenarios.
 102

2 RELATED WORK

103 **Data Efficiency.** Large-scale datasets have enabled neural networks to achieve unprecedented suc-
 104 cess (Kaplan et al., 2020; Li et al., 2025). However, training on massive data comes at a high cost:
 105 it requires substantial computational resources, consumes substantial energy, and produces a mas-
 106 sive amount of carbon footprint (Strubell et al., 2020; Patterson et al., 2021). Moreover, we are
 107 approaching practical and economic limits on collecting more data for training (Villalobos et al.,
 108 2022; Muennighoff et al., 2023). To address these challenges, a substantial body of work focused
 109 on data selection strategies (Xia et al., 2024; Xie et al., 2023; Gu et al., 2024; Albalak et al., 2024;

108 Yu et al., 2024). Most such approaches optimize data efficiency by selecting training examples according to various utility measures, e.g., quality and contribution to training loss reduction. Some 109 studies suggest that data diversity can be equally important, but most existing work treats diversity 110 as a broad and generic concept, typically defining and quantifying it in the embedding space using 111 similarity-based measures (Friedman & Dieng, 2022; Miranda et al., 2023; Zhang et al., 2024). 112 However, diversity can take multiple forms (Rahimi et al., 2023), such as semantic and structural 113 diversity, which may influence not only how well a model fits the training set, but also how effectively 114 it can extrapolate to novel combinations. 115

116 **Compositional Generalization.** Systematic compositionality is the ability of recombination of 117 known parts and rules (Hupkes et al., 2020; Wiedemer et al., 2023), which is a feature of human 118 cognition (Frankland & Greene, 2020; Dehaene et al., 2022; Elmoznino et al., 2024). Inspired 119 by this, a growing body of work has emerged to analyze the compositionality of data (Wiedemer 120 et al., 2023), the compositional generalization ability of machine learning models (Dziri et al., 2023; 121 Ramesh et al., 2023; Lake & Baroni, 2023), as well as the process by which these abilities emerge 122 during training (Park et al., 2024; Yang et al., 2024; Okawa et al., 2023). In particular, Park et al. 123 (2024) and Okawa et al. (2023) used diffusion models to show that the emergence of compositional 124 ability involved two stages. Model first disentangles individual components, and then it manipulates 125 and recombines them to produce novel outputs. In this work, we focus on transformer-based 126 models (Vaswani et al., 2017), as they form the backbone of most state-of-the-art AI systems. Al- 127 though some studies have argued that transformers lack compositional generalization abilities (Dziri 128 et al., 2023), these primarily focus on productive compositional generalization ability (Ramesh et al., 129 2023), which often requires generalizing to longer or more complex examples than those observed 130 during training (Hupkes et al., 2020). By contrast, our work centers on systematic compositional 131 generalization, emphasizing the model’s ability to generalize to novel combinations of known 132 components with known rules. [Recent studies also investigated the impact of data diversity on compositional generalization, finding that increased diversity is beneficial \(Zhou et al., 2023; Akyürek & Andreas, 2022; Uselis et al., 2025\).](#) Our work extends these findings by formally distinguishing 133 and theoretically separating semantic diversity and structural diversity. This formal decomposition 134 allows us to derive explicit generalization error bounds. 135

3 DATA-DRIVEN COMPOSITIONAL GENERALIZATION

138 To formalize data diversity from the perspective of compositionality, let the input space be \mathcal{X} and 139 output space be \mathcal{Y} , and \mathbb{C} represents the set of compositional structures in training dataset. Each 140 data instance can be disentangled into a structure and an input. A structure is denoted by f_c (e.g., 141 $x_1 \times x_2 + x_3$ in algebraic circuits as A and C in Figure 1), where $c \in \mathbb{C}$ specifies the composition. 142 The inputs $\{x_{c,m}, \forall c \in \mathbb{C}, m \in [M]\}$ provide concrete instantiations of structures (e.g., $1 \times 5 + 6$ 143 in Figure 1), where $[M] = \{1, 2, \dots, M\}$, and yield data instances $(f_c(x_{c,m}), y_{c,m}) \in \mathcal{X} \times \mathcal{Y}$ (e.g., 144 $(1 \times 5 + 6, 11)$). Furthermore, each structure f_c can be decomposed into components. 145 Formally, let \mathcal{S} denote the pool of components, then the structure can be expressed as $f_c(x_{c,m}) = 146 c(s_1(x_{c,m}), s_2(x_{c,m}), \dots, s_t(x_{c,m}))$, where $s_i \in \mathcal{S}$ are the components, while the composition rule 147 c specifies how these components are combined. In algebraic circuits (Ito et al., 2024; Savage, 1998), 148 for example, each $s_i(\cdot)$ may correspond to a sub-circuit (e.g., $x_1 \times x_2$). 149

150 The training dataset $\mathbb{D} = \{\{(f_c(x_{c,m}), y_{c,m})\}_{\forall m \in [M]}\}_{\forall c \in \mathbb{C}}$ consists of $N = |\mathbb{C}|$ distinct 151 compositions, and each instantiated M times with different inputs. The data budge is $K = M \cdot N$, cor- 152 responding to the number of training examples. In this framework, structural diversity is captured 153 by N , while semantic diversity is captured by M . This setup explicitly connects data diversity to 154 the two fundamental aspects of compositionality: components and combinations. Let \mathbb{D}_c denote the 155 set of all possible data consistent with the same underlying compositional structure c , and for the 156 structure c , the training dataset has $\mathbb{D}'_c = \{(f_c(x_{c,m}), y_{c,m})\}_{\forall m \in [M]} \subset \mathbb{D}_c$, which is also a subset 157 of the overall training dataset \mathbb{D} . The loss function $l(\cdot)$ is L -Lipschitz and bounded by λ . 158

3.1 ACQUIRE UNDERLYING COMPONENTS

159 An essential step toward compositional generalization is learning the components that constitute a 160 structure, since these components form the basis of data-generating process Wiedemer et al. (2023). 161 Given a dataset $\mathbb{D}'_c \subset \mathbb{D}_c$ consisting of M different surface realizations of the same structure (se- 162 mantic diversity), a model can decompose and learn the basic components (Park et al., 2024). The

162 generalization error on \mathbb{D}_c primarily reflects the model's ability to learn these underlying components,
 163 since f_c is fixed. One way to analyze the generalization error is through Rademacher complexity
 164 (Shalev-Shwartz & Ben-David, 2014), which provides a theoretical measure of the expressiveness
 165 of a hypothesis class and thus yields a bound on its generalization performance.

166 By standard results in statistical learning theory, the generalization error of a hypothesis class \mathcal{H}
 167 within \mathbb{D}_c is bounded in terms of its empirical error on \mathbb{D}'_c , the empirical Rademacher complexity,
 168 and the number of training examples $M = |\mathbb{D}'_c|$:

$$170 \quad \text{err}_{\mathbb{D}_c}(h) \leq \text{err}_{\mathbb{D}'_c}(h) + 2 \cdot \text{Rad}_{\mathbb{D}'_c}(l \circ \mathcal{H}) + 4\lambda \sqrt{\frac{2 \ln 4/\delta}{M}}, \quad (1)$$

172 with probability of at least $1 - \delta$ for all hypotheses $h \in \mathcal{H}$. Here, $\text{err}_{\mathbb{D}_c}(h) = \mathbb{E}_{\mathbb{D}_c} l(h(f_c(x)), y_c)$
 173 is the intra-compositional generalization error, $\text{err}_{\mathbb{D}'_c}(h) = \frac{1}{M} \sum_{m=1}^M l(h(f_c(x_{c,m})), y_{c,m})$ is the
 174 empirical error on the training dataset, and $\text{Rad}_{\mathbb{D}'_c}(l \circ \mathcal{H})$ is the empirical Rademacher complexity
 175 of the hypothesis class. This is detailed in Appendix B.

177 When the empirical error $\text{err}_{\mathbb{D}'_c}(h)$ is small, e.g., when the model can fit the training dataset well, the
 178 intra-compositional generalization error can be bounded primarily by the Rademacher complexity
 179 and the number of training examples M . In particular, if $0 < \text{err}_{\mathbb{D}'_c}(h) < \xi$ for any $\xi > 0$, we have:

$$181 \quad \text{err}_{\mathbb{D}_c}(h) \leq \xi + 2\text{Rad}_{\mathbb{D}'_c}(l \circ \mathcal{H}) + 4\lambda \sqrt{\frac{2 \log 4/\delta}{M}}. \quad (2)$$

183 Let $\mathcal{A} \subset \mathbb{R}^M$ denotes a set of vectors $\mathcal{A} = \{[h(f_c(x_{c,1})), \dots, h(f_c(x_{c,M}))] \in \mathbb{R}^M | h \in \mathcal{H}\}$, which
 184 lies in an r -dimensional subspace of \mathbb{R}^M and such that $\alpha = \max_{\mathbf{a} \in \mathcal{A}} \|\mathbf{a}\|$. We use r to characterize
 185 the semantic complexity, i.e., the internal variability of each component. For instance, in algebraic
 186 circuits, a deeper sub-circuit allows for a wider range of distinct surface realizations, leading to a
 187 larger r . Shown in Anthony & Bartlett (2009) and Shalev-Shwartz & Ben-David (2014), in this case,
 188 the Rademacher complexity satisfies:

$$190 \quad \text{Rad}_{\mathbb{D}'_c}(l \circ \mathcal{H}) \leq \frac{6\alpha}{M} (\sqrt{r \log(2\sqrt{r})} + 2\sqrt{r}) = O\left(\frac{\alpha\sqrt{r \log r}}{M}\right). \quad (3)$$

192 Combining these results, we could yield an explicit upper bound of the intra-compositional generalization error in Theorem 3.1.

194 **Theorem 3.1** (Bound of Intra-Compositional Generalization Error). *Let \mathcal{H} be a hypothesis class,
 195 and suppose the loss function $l(\cdot)$ is L -Lipschitz and bounded by λ . Assume the empirical loss
 196 satisfies $0 < \text{err}_{\mathbb{D}'_c} < \xi$ for any $\xi > 0$. Let $\mathcal{A} \subset \mathbb{R}^M$ denotes a set of vectors, $\mathcal{A} =$
 197 $\{[h(f_c(x_{c,1})), \dots, h(f_c(x_{c,M}))] \in \mathbb{R}^M | h \in \mathcal{H}\}$, lies in an r -dimensional subspace in \mathbb{R}^M , where
 198 r characterizes the complexity of the underlying components, and $\alpha = \max_{\mathbf{a} \in \mathcal{A}} \|\mathbf{a}\|$. Then, with
 199 probability at least $1 - \delta$, the intra-compositional generalization error for all hypotheses $h \in \mathcal{H}$ is
 200 bounded by:*

$$201 \quad O\left(\frac{\alpha\sqrt{r \log r}}{M} + \lambda \sqrt{\frac{\log 1/\delta}{M}}\right).$$

204 3.2 GENERALIZE TO UNSEEN COMBINATIONS

206 Once a model has robustly learned individual components, a critical step is to learn to recombine
 207 them into novel compositional functions defined with respect to these components. This is often
 208 referred to as systematic compositional generalization (Hupkes et al., 2020). Achieving systematic
 209 compositional generalization requires learning to recombine components into novel functions. Since
 210 the process involves generalizing to unseen compositional structures, we bound this generalization
 211 error with covering number (Anthony & Bartlett, 2009) over the space of all possible compositions.

212 Assume that all possible compositional functions in \mathbb{C}_{all} (the set of compositional functions in the
 213 training dataset is a subset $\mathbb{C} \subset \mathbb{C}_{\text{all}}$) can be embedded into a d -dimensional space \mathcal{V} by an embedding
 214 function $\phi(\cdot)$, where each point in \mathcal{V} (i.e., $\phi(c')$ and $c' \in \mathbb{C}_{\text{all}}$) represents a specific combination
 215 of learned components, and distances between points in the space reflect the similarity between compositions. The space \mathcal{V} is modeled as a d -dimensional Euclidean space, which is applied to the latent

representation $\phi(\cdot)$ and enables tractable geometric analysis. We use d to characterize the structural complexity, i.e., the diversity of possible combinations of components. For example, a composition with more layers allows for a greater combinatorial richness of arrangements, resulting in a larger d . Under this assumption, if a model \mathcal{M}_θ (e.g., a hypothesis $h \in \mathcal{H}$) is trained on a dataset containing a particular compositional function $c \in \mathbb{C}$, it is expected to generalize more easily to similar compositions, i.e., those $c' \in \mathbb{C}_{\text{all}}$ satisfying $\|\phi(c) - \phi(c')\| \leq \epsilon$ for some threshold $\epsilon > 0$. Furthermore, the generalization performance on c' degrades with $\|\phi(c) - \phi(c')\|$. For example, suppose the training composition corresponds to the circuit $c_1(\cdot) = ((x_1 + x_2) + x_3) \cdot x_4$, and a structurally similar variant such as $c_2(\cdot) = (x_1 + (x_2 + x_3)) \cdot x_4$ satisfies $|\phi(c_1) - \phi(c_2)| \leq \epsilon$. In contrast, a structurally distant variant such as $c_3(\cdot) = (x_1 + x_2) \cdot (x_3 + x_4)$ satisfies $|\phi(c_1) - \phi(c_3)| > \epsilon$. Although the true conceptual space may be more complex, modeling it as a d -dimensional Euclidean space enables tractable geometric analysis. In this view, each composition observed during training defines an ϵ -radius ball in the space \mathcal{V} , representing the region over which \mathcal{M}_θ can generalize from $c \in \mathbb{C}$ with generalization error smaller than ϵ , i.e., $\text{err}_c(c') \leq \epsilon$, where $\text{err}_c(c') = \mathbb{E}_{\mathbb{D}_{c'}} l(\mathcal{M}_\theta(f_{c'}(\cdot)), y_{c'})$. So, the radius ϵ serves as an upper bound of inter-compositional generalization error.

Training on $N = |\mathbb{C}|$ distinct compositions corresponds to covering the space with N ϵ -radius balls. As N increases, the space \mathcal{V} can be covered using balls with smaller radius ϵ , implying that a larger training set permits finer granularity in coverage and reduces the upper bound of inter-compositional generalization error. Conversely, when N is small, a larger ϵ is required for coverage, which leads to higher inter-compositional generalization error. Minimizing N while keeping ϵ small captures the trade-off between data efficiency and inter-compositional generalization in our framework. Formally, the covering number ($N(\epsilon, \mathcal{V}, \|\cdot\|)$) is defined as the minimal number of balls (under norm $\|\cdot\|$) required to cover the space \mathcal{V} . This notion can be used to establish a relationship between the error bound ϵ and the number of distinct compositions N . This is detailed in Appendix C.

From standard results in statistics (Shalev-Shwartz & Ben-David, 2014; Mohri et al., 2018), the covering number N can be bounded as a function of the space dimension d , which could be used to characterize the compositional complexity, and the radius ϵ as $N \leq (\frac{2}{\epsilon} + 1)^d$. This could be rearranged to express the effect of number of compositions provided in training set, i.e., N , on the upper bound of the inter-compositional generalization error, i.e., ϵ :

$$\text{err}_{\mathbb{C}_{\text{all}}} \leq \epsilon \leq \frac{2}{N^{\frac{1}{d}} - 1}. \quad (4)$$

We formalize this in Theorem 3.2.

Theorem 3.2 (Bound of Inter-Compositional Generalization Error). *Let the set of all possible compositions \mathbb{C}_{all} form a conceptual space \mathcal{V} , modeled as a d -dimensional Euclidean norm ball, where d characterizes the compositional complexity. Assume each composition observed during training covers an ϵ -radius ball in this space, within which the inter-compositional generalization error $\text{err}_{\mathbb{C}_{\text{all}}}$ is at most ϵ . Then, the inter-compositional generalization error can be bounded by:*

$$O\left(\frac{1}{N^{\frac{1}{d}} - 1}\right),$$

where N is the number of distinct compositions presented in the training data.

3.3 ROLE OF DATA DIVERSITY IN COMPOSITIONAL GENERALIZATION

We established upper bounds for both intra-compositional and inter-compositional generalization error in Theorem 3.1 and Theorem 3.2, respectively, and the results connect directly to the two dimensions of data diversity discussed earlier. The overall error bound of generalization error from the perspective of compositions can be expressed as the summation of these two:

$$\text{err} = O\left(\frac{\alpha\sqrt{r \log r}}{M} + \lambda\sqrt{\frac{\log 1/\delta}{M}} + \frac{1}{N^{\frac{1}{d}} - 1}\right). \quad (5)$$

Here, the first two terms depend on semantic diversity through M , capturing the model's ability to generalize across variations of the same underlying structure (e.g., A-C in Figure 1); while the last term depends on structural diversity through N , capturing its ability to generalize to new combinations (e.g., A-B in Figure 1). We combine these two error bounds by addition, reflecting the

270 decomposition where minimizing the total error requires robust component learning and effective
 271 generalization across structures. Achieving zero error in one component does not imply perfect gen-
 272 eralization overall, justifying the additive model. For simplicity, we omit potential coupling terms
 273 in our analysis, and detailed discussion is provided in Appendix A.

274 Given a fixed data budget $K = M \cdot N$, the overall generalization error could be upper bounded by
 275 the term of N , the number of distinct compositions exposing during training:

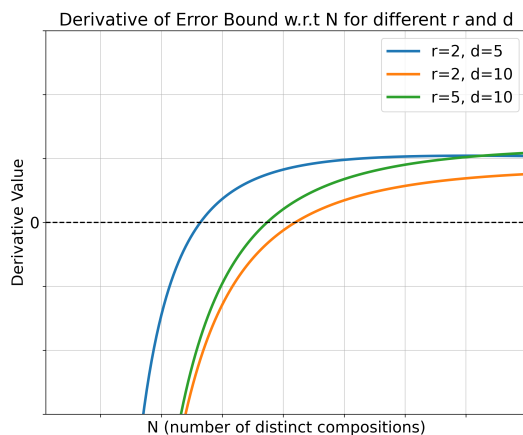
$$277 \text{err} = O(\mathcal{F}(N, r, d)), \quad \text{s.t. } \mathcal{F}(N, r, d) = O\left(\frac{N\alpha\sqrt{r\log r}}{K} + \lambda\sqrt{\frac{N\log 1/\delta}{K}} + \frac{1}{N^{\frac{1}{d}} - 1}\right). \quad (6)$$

278 Equation 6 illustrates that different aspects of data diversity affect the generalization error bound in
 279 opposite ways under a fixed data budget. Specifically, in the first two terms, increasing N enlarges
 280 the error bound. In contrast, the last term decreases with N , as additional compositions improve
 281 structural coverage. This demonstrates that increasing diversity without a principled strategy does
 282 not necessarily lead to optimal generalization ability, and the training dataset requires a balanced
 283 allocation between semantic and structural diversity to achieve data efficiency.

284 To further investigate how different aspects of diversity influence the generalization performance,
 285 we differentiate the bound in Equation 6 with respect to N . This yields:

$$288 \frac{\partial \mathcal{F}(\cdot)}{\partial N} = \frac{\alpha\sqrt{r\log r}}{K} + \frac{\lambda\zeta}{2\sqrt{\zeta N}} - \frac{N^{\frac{1}{d}-1}}{d(N^{\frac{1}{d}} - 1)^2}, \quad \text{s.t. } \zeta = \frac{\log 1/\delta}{K}. \quad (7)$$

289 As illustrated in Figure 2, once N exceeds a point N^* , introducing additional distinct compositions
 290 leads to an increase in the error bound. Moreover, both the component complexity (cap-
 291 tured by r) and the compositional complexity (captured by d) have a significant effect on the
 292 derivative and thus influence the increasing or decreasing trend of the error bound. While the
 293 stationary points N^* may appear close in the illustrative figure, in practice different r and d val-
 294 ues can induce substantial shifts in N^* . These results are summarized formally in Theorem 3.3.



305 Figure 2: Derivative of the generalization error
 306 bound with respect to N under varying levels of
 307 component complexity r and compositional com-
 308 plexity d . When the derivative is negative, adding
 309 more distinct compositions N decreases the error
 310 bound, whereas once it becomes positive, further
 311 increasing N causes the error bound to rise. Both
 312 r and d influence the threshold (stationary point)
 313 at which the transition occurs.

314 data budget. Specifically, when N^* is small, which corresponds to high component complexity,
 315 the regime $N > N^*$ is more prevalent. In this case, increasing semantic diversity, i.e., providing
 316 more realizations per composition structure, contributes more effectively. In contrast, when N^* is
 317 large, corresponding to low component complexity and a compositionality bottleneck, the regime

Theorem 3.3 (Monotonicity of the Generalization Error Bound). *The bound $\mathcal{F}(N, r, d)$ be-
 318 defined as in Equation 6 under a fixed data bud-
 319 get $K = M \cdot N$. Here, r characterizes the
 320 component complexity and d characterizes the
 321 compositional complexity. Then, the following
 322 monotonicity properties hold with respect to N :*

- (i) *There exists a stationary point $N^* > 1$, such that $\mathcal{F}(N, r, d)$ is strictly decreasing for $N < N^*$ and strictly increasing for $N > N^*$.*
- (ii) *The stationary point N^* decreases as r increases, i.e., higher component complexity. More semantic diversity will provide more benefits when the dataset has higher component complexity.*
- (iii) *The stationary point N^* increases as d increases, i.e., greater compositional complexity and lower component complexity. More structural diversity will provide greater benefits when the dataset has higher compositional complexity.*

323 Our analysis does not aim to determine the exact value of the optimal N^* , but rather to char-
 324 acterize the monotonic behavior and provide high-level guidance for allocating the two di-
 325 mensions of data diversity under constrained

324 $N < N^*$ is more common. In this case, increasing structural diversity, i.e., exposing more distinct
 325 compositions, has a greater impact on improving generalization.
 326

327 4 EMPIRICAL EVALUATION

328
 329 We empirically evaluate our theoretical framework, beginning with fully controlled synthetic
 330 datasets to real-world data. Our goal is to investigate whether the two dimensions of data diversity
 331 introduced in our framework manifest in practice, and in particular, to validate whether the proposed
 332 allocation strategy leads to improved generalization or more data-efficient training. **We emphasize**
 333 **that this approach is fundamentally different from existing data selection or argumentation strategies.**
 334 **Our framework, in contrast, proposes structural design principles based on inherent task properties**
 335 **and diversity.** We begin with synthetic algebraic circuits, employing both a small-scale encoder-
 336 only model and large language models (LLMs) such as GPT-2-XL (Brown et al., 2020) and Mistral
 337 7B v0.1 (Jiang et al., 2023). This experimental design enables precise control over data diversity,
 338 allowing us to examine how models behave under different allocations of semantic and structural
 339 diversity, and it further highlights the role of model capacity and task difficulty affect the results, cor-
 340 responding to the component complexity and compositional complexity introduced in Theorem 3.3.
 341 We then validate our framework on a real-world dataset GSM8K (Cobbe et al., 2021), which can be
 342 naturally represented as circuit structures, using Mistral 7B v0.1 (Jiang et al., 2023) to assess our
 343 findings under realistic settings. Although the models we employ are not among the most recent,
 344 we deliberately choose them because state-of-the-art models already achieve strong performance,
 345 making additional fine-tuning or training less informative for assessing the impact of data diversity.
 346

347 4.1 SYNTHETIC SETUP

348 This setting provides full controllability over both semantic and structural diversity, enabling a direct
 349 test of our theoretical framework. Each circuit corresponds to an algebraic expression such as $4 \times (5 \times$
 350 $2 + 5)$. By computing the result modulo 10, the problem becomes a modular arithmetic. We further
 351 introduce variability through sub-circuits to control the component complexity. By adjusting circuit
 352 structure, sub-circuit depth, number of distinct structures (N), and number of realizations of the
 353 same underlying structure (M), we can systematically vary both semantic and structural diversity, as
 354 well as the component and structural complexity. The dataset is constructed by K training examples,
 355 where $K = M \cdot N$. Thus, structural diversity is determined by N , while semantic diversity is
 356 determined by M . This is detailed in Appendix G. We consider two types of model here: (i) training
 357 an encoder-only model from scratch, and solve each circuit as a 10-classes classification problem (ii)
 358 fine-tune a pretrained large language model, where both the final answer and the chain-of-thought
 359 (CoT) are provided in the training dataset, an example is shown in Appendix D. This effectively
 360 guides the model to perform an explicit decomposition during training.

361 4.1.1 ENCODER-ONLY MODEL

362 We first use an encoder-only model trained from scratch on the synthetic dataset. The model is imple-
 363 mented as a one-layer transformer block with a standard embedding layer, a multi-head self-attention
 364 layer, and a feed-forward layer. The model’s architecture and the training hyperparameters are de-
 365 tailed in Appendix D.1. We monitor the loss on the testing set, in which each circuit is composed of
 366 the same set of sub-circuits as those in the training dataset, but arranged into novel compositional
 367 structures. This design enables us to evaluate the model’s ability to generalize to novel structures
 368 composed of previously learned components.

369 Figure 3 shows evaluation loss curves of the one-layer transformer under different allocations of
 370 semantic and structural diversity (M and N), with a fixed data budget $K = 10,000$. When the
 371 components are simple (r is small; e.g., 1-layer sub-circuit and overall depth 3), generalization is
 372 primarily constrained by recombination. In this regime, the stationary point N^* in the error bound
 373 becomes large, meaning that models often operate in the range $N < N^*$. As a result, increasing
 374 structural diversity (i.e., raising N) leads to improved performance, while models trained with
 375 limited structural diversity tend to plateau at higher loss. In contrast, when components are more
 376 complex (r is large; e.g., 2-layer sub-circuit with overall depth 3), the regime $N > N^*$ becomes
 377 more likely, and the benefits of increasing structural diversity diminish or even disappear, as re-
 378 flected by the narrowing of loss curves across different values of N . This indicates that as sub-

circuits become harder to learn, the bottleneck shifts from recombination to component acquisition, and the stationary point N^* shifts left as in Figure 2. Taken together, these results highlight a key aspect of our theoretical framework: a model’s ability to achieve systematic compositional generalization depends on both acquiring individual components and learning how to recombine them. When components are relatively simple, greater structural diversity (i.e., more distinct compositions) is beneficial, as the challenge lies in learning how to recombine components. Conversely, when components are more complex, increasing semantic diversity (i.e., providing more surface realizations per composition) becomes more effective, as the bottleneck lies in learning the components themselves.

4.1.2 LARGE LANGUAGE MODELS

We evaluate LLMs, specifically GPT-2-XL (1.5B) (Brown et al., 2020) and Mistral 7B v0.1 (7B) (Jiang et al., 2023), on the synthetic algebraic circuits dataset. For these models, we additionally provide CoT reasoning traces for solving the problems, as shown in Appendix D. Using LLMs serves two purposes: (i) to examine whether our theoretical framework holds when applied to large-scale models, and (ii) to investigate how model capacity influences these insights. In particular, we study how the component complexity (r in Theorem 3.3) shifts as model capacity increases. Intuitively, higher-capacity models are able to solve the same components with greater ease, such that component complexity decreases. This allows us to connect the theoretical framework to pretrained models, thereby providing evidence that our findings extend beyond small-scale settings. These models may already encode compositional patterns and reasoning skills due to their large-scale pretraining. This prior knowledge could potentially reduce the marginal benefit of additional diversity in the fine-tuning stage. However, we deliberately chose to use non-state-of-the-art models for fine-tuning because they offer a clearer window into observing the impact of the data diversity on generalization.

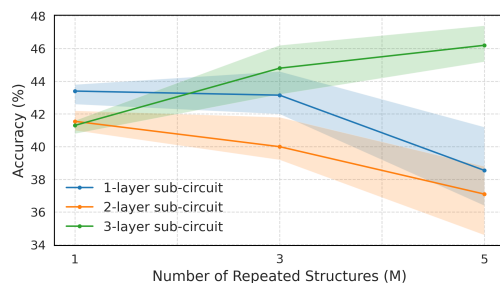


Figure 4: Performance of GPT-2-XL fine-tuned on algebraic circuits with different levels of semantic diversity (M). Results are shown for circuits of overall depth 4. Increasing semantic diversity improves accuracy when component complexity is high, but can degrade performance at low sub-circuit complexity.

In Figure 4 and Figure 5, We report 5 independent runs, including data sampling, training and inference. Solid lines denote the average performance, and shaded regions indicate the range across runs. Figure 4 shows the test accuracy of GPT-2-XL fine-tuned with a fix data budget $K = 4,500$ with CoT, tested on a set of 500 distinct circuits that do not overlap with the training data. When

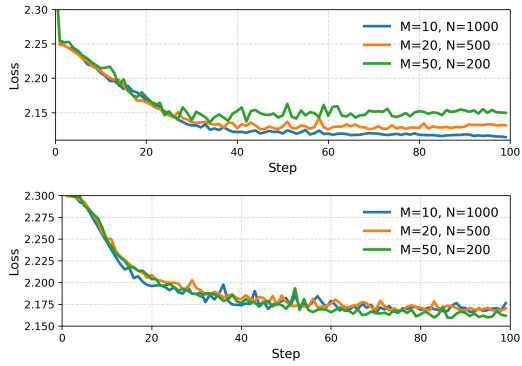


Figure 3: *Top*: Evaluation loss curve for circuits with 1-layer sub-circuits and overall depth 3. Structural diversity plays a dominant role, with higher N (number of distinct compositions) yielding lower loss. *Bottom*: Evaluation loss curve for circuits with 2-layer sub-circuits and overall depth 3. As component complexity increases, the performance gap across different values of N narrows.

ity models are able to solve the same components as the baseline model as the number of components decreases. This allows us to connect the theoretical findings to the empirical results, providing evidence that our findings extend beyond the baseline model. **Decoding compositional patterns and reasoning skills** We hypothesize that the knowledge of the components and how they interact could potentially reduce the marginal impact of the components on the final output. However, we deliberately chose to use non-linear models to ensure that the components do not offer a clearer window into observing the impact of the components on the final output.

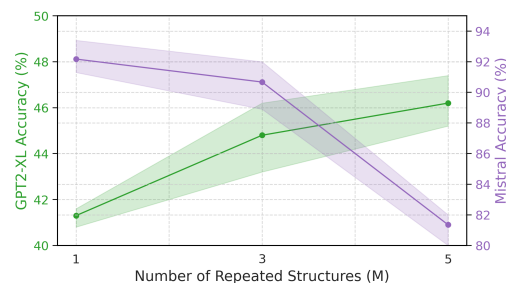


Figure 5: Performance of GPT-2-XL (1.5B) and Mistral (7B) fine-tuned on algebraic circuits with varying levels of semantic diversity (M). For GPT-2 XL, increasing semantic diversity improves performance, whereas the opposite trend is observed for Mistral: higher semantic diversity degrades performance.

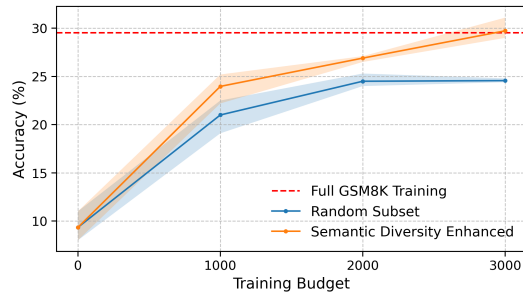
432 the components are relatively simple (r is small, e.g., 1-layer and 2-layer sub-circuits), increasing
 433 semantic diversity (i.e., increasing M and decreasing N) offers no benefits and may even reduce
 434 performance, as the stationary point N^* is large and N lies below the threshold, i.e., $N < N^*$ with
 435 high probability. In contrast, when the components are more difficult (r is large, e.g., 3-layer sub-
 436 circuits), increasing semantic diversity yields better performance, as the stationary point N^* shifts
 437 to a smaller value, and models typically operate in the regime $N > N^*$, where additional semantic
 438 diversity is more beneficial. Thus decreasing N moves the allocation towards N^* and improves
 439 performance. Next, we extend our study on Mistral (7B), which is substantially larger, and more
 440 powerful than GPT-2-XL. We fine-tune Mistral using the dataset with 3-layer sub-circuits. As shown
 441 in Figure 5, increasing semantic diversity harms performance for Mistral. Compared to GPT-2-XL,
 442 Mistral’s greater capacity suggests that each component is easier for it to learn, i.e., the component
 443 difficulty r is lower for Mistral. According to Theorem 3.3, as r decreases, the stationary point N^*
 444 increases and shifts to larger values. Under a fixed training budget K , increasing M and reducing
 445 N , shifts the data allocation away from the optimal, leading to degraded performance. These results
 446 indicate that simply increasing one form of diversity does not guarantee optimal performance; in-
 447 stead, the ideal allocation depends on both the task characteristics and the model’s capacity. This
 448 further demonstrates that our theoretical framework offers practical guidance for fine-tuning large,
 449 pretrained models.

450 4.2 REAL DATA

451 To validate our framework beyond synthetic
 452 settings, we apply it to real-world data. Mathematical problems can naturally be abstracted
 453 into circuit-like structures as detailed in Appendix F, where each problem is decomposed
 454 into functional components. The problems in
 455 GSM8K dataset are essentially shallow circuits:
 456 most questions require only one or two layers of
 457 composition, but solving each sub-step is non-
 458 trivial for models, as it involved not only car-
 459 rying out basic operations but also understand-
 460 ing and formalizing the problem statement. In
 461 our framework, this corresponds to low compo-
 462 sitional complexity (d is small) and high com-
 463 ponent complexity (r is large), suggesting that
 464 semantic diversity is more critical, since deep
 465 compositional reasoning is rarely required.

466 We use GPT-4o (Hurst et al., 2024) to generate
 467 GSM-style examples. The generated examples
 468 follow the same underlying reasoning paths as
 469 the original one in GSM8K dataset but differ in
 470 their surface realization, thereby enriching se-
 471 mantic diversity without altering compositional structure. The prompts used for generating GSM-
 472 style examples, and example outputs are provided in Appendix E. We then fine-tune Mistral on two
 473 different data configurations: (i) a random subset, in which we use examples randomly sampled
 474 from GSM8K (resulting in higher structural diversity, i.e., larger N), and (ii) a semantic diversity
 475 enhanced dataset, in which we have pairs data where each GSM8K seed example is accompanied
 476 by a semantically diverse variant with identical reasoning structure (smaller N), as shown in Ap-
 477 pendix E. The structural diversity is intentionally reduced in configuration (ii), allowing us to study
 478 the impact of this shift in diversity allocation. In both cases, we control the total training budget.
 479 For example, if the budget $K = 5,000$, configuration (i) uses 5,000 randomly selected GSM8K
 480 problems, while configuration (ii) uses 2,500 seed examples and 2,500 GPT-4o-generated variants.

481 Figure 6 compares the performance of fine-tuned models under different training data budget.
 482 Across all budget levels, subsets curated to enhance semantic diversity consistently outperform size-
 483 matched random subsets. Remarkably, with only 3,000 training examples, the semantic diversity-
 484 enhanced setting matches or even exceeds the accuracy achieved by fine-tuning on the full GSM8K
 485 dataset. In this regime, components complexity is relatively high (r is large), while compositional



486 Figure 6: Model performance under different
 487 training budgets. We compare randomly sam-
 488 pled subsets of GSM8K to a semantic diversity-
 489 enhanced setting, where each seed example is
 490 paired with a semantically diverse variant of iden-
 491 tical reasoning structure. We report the results of 4
 492 independent runs, including data sampling, train-
 493 ing, and inference. Solid lines denote the aver-
 494 age performance, and shaded regions indicate the
 495 range across runs.

496 9

486 complexity remains low (d is small). According to Theorem 3.3, the stationary point N^* is there-
 487 fore small. Reducing structural diversity (N) in this context moves the diversity allocation closer to
 488 N^* , leading to improved performance. This finding suggests that identifying an effective balance
 489 between semantic and structural diversity can significantly enhance a model’s ability to generalize
 490 to unseen data in a data-efficient manner.

491 **5 CONCLUSION**

494 In this work, we analyzed the role of data diversity through the lens of compositional generaliza-
 495 tion and explore how it can enable more data-efficient learning. We refined the broad concept of
 496 diversity into two complementary dimensions: semantic diversity, which supports the acquisition of
 497 underlying components, and structural diversity, which enables generalization to unseen composi-
 498 tions. Our theoretical framework demonstrates that these two dimensions influence generalization
 499 in different ways, and further reveals that under a constrained data budget, the optimal balance be-
 500 tween them depends on both component complexity and compositional complexity. Experiments
 501 on synthetic datasets validated the framework and highlighted the role of model capacity in shift-
 502 ing the optimal allocation. Results on GSM8K further confirmed the framework’s applicability to
 503 real-world problems. Overall, our findings highlight the critical role of data diversity and provide a
 504 principled strategy for constructing datasets that enable more data-efficient and generalizable train-
 505 ing. A direction for future research is to extend this theoretical framework to other mathematical
 506 and logical settings, incorporating the new diversity dimensions and types of compositionality that
 507 those domains would naturally introduce.

508 **REFERENCES**

510 Ekin Akyürek and Jacob Andreas. Compositionality as lexical symmetry. *arXiv preprint arXiv:2201.12926*, 2022.

512 Alon Albalak, Yanai Elazar, Sang Michael Xie, Shayne Longpre, Nathan Lambert, Xinyi Wang, Niklas Muennighoff, Bairu Hou, Liangming Pan, Haewon Jeong, et al. A survey on data selection for language models. *arXiv preprint arXiv:2402.16827*, 2024.

516 Martin Anthony and Peter L Bartlett. *Neural network learning: Theoretical foundations*. cambridge university press, 2009.

518 Tom Brown, Benjamin Mann, Nick Ryder, Melanie Subbiah, Jared D Kaplan, Prafulla Dhariwal, Arvind Neelakantan, Pranav Shyam, Girish Sastry, Amanda Askell, et al. Language models are few-shot learners. *Advances in neural information processing systems*, 33:1877–1901, 2020.

522 Noam Chomsky. *Aspects of the Theory of Syntax*. MIT press, 2014.

524 Karl Cobbe, Vineet Kosaraju, Mohammad Bavarian, Mark Chen, Heewoo Jun, Lukasz Kaiser, Matthias Plappert, Jerry Tworek, Jacob Hilton, Reiichiro Nakano, et al. Training verifiers to solve math word problems. *arXiv preprint arXiv:2110.14168*, 2021.

527 Stanislas Dehaene, Fosca Al Roumi, Yair Lakretz, Samuel Planton, and Mathias Sablé-Meyer. Symbols and mental programs: a hypothesis about human singularity. *Trends in Cognitive Sciences*, 26(9):751–766, 2022.

531 Prafulla Dhariwal and Alexander Nichol. Diffusion models beat gans on image synthesis. *Advances in neural information processing systems*, 34:8780–8794, 2021.

533 Andrew Drozdzov, Nathanael Schärli, Ekin Akyürek, Nathan Scales, Xinying Song, Xinyun Chen, Olivier Bousquet, and Denny Zhou. Compositional semantic parsing with large language models. *arXiv preprint arXiv:2209.15003*, 2022.

537 Nouha Dziri, Ximing Lu, Melanie Sclar, Xiang Lorraine Li, Liwei Jiang, Bill Yuchen Lin, Sean Welleck, Peter West, Chandra Bhagavatula, Ronan Le Bras, et al. Faith and fate: Limits of transformers on compositionality. *Advances in Neural Information Processing Systems*, 36:70293–70332, 2023.

540 Eric Elmoznino, Thomas Jiralerpong, Yoshua Bengio, and Guillaume Lajoie. A complexity-based
 541 theory of compositionality. *arXiv preprint arXiv:2410.14817*, 2024.

542

543 Steven M Frankland and Joshua D Greene. Concepts and compositionality: in search of the brain's
 544 language of thought. *Annual review of psychology*, 71(1):273–303, 2020.

545

546 Dan Friedman and Adji Bousoo Dieng. The vendi score: A diversity evaluation metric for machine
 547 learning. *arXiv preprint arXiv:2210.02410*, 2022.

548

549 Aaron Grattafiori, Abhimanyu Dubey, Abhinav Jauhri, Abhinav Pandey, Abhishek Kadian, Ahmad
 550 Al-Dahle, Aiesha Letman, Akhil Mathur, Alan Schelten, Alex Vaughan, et al. The llama 3 herd
 551 of models. *arXiv preprint arXiv:2407.21783*, 2024.

552

553 Thomas L Griffiths. Understanding human intelligence through human limitations. *Trends in Cognitive Sciences*, 24(11):873–883, 2020.

554

555 Yuxian Gu, Li Dong, Hongning Wang, Yaru Hao, Qingxiu Dong, Furu Wei, and Minlie Huang. Data
 556 selection via optimal control for language models. *arXiv preprint arXiv:2410.07064*, 2024.

557

558 Daya Guo, Dejian Yang, Haowei Zhang, Junxiao Song, Ruoyu Zhang, Runxin Xu, Qihao Zhu,
 559 Shirong Ma, Peiyi Wang, Xiao Bi, et al. Deepseek-r1: Incentivizing reasoning capability in llms
 560 via reinforcement learning. *arXiv preprint arXiv:2501.12948*, 2025.

561

562 Irina Higgins, Loic Matthey, Arka Pal, Christopher Burgess, Xavier Glorot, Matthew Botvinick,
 563 Shakir Mohamed, and Alexander Lerchner. beta-vae: Learning basic visual concepts with a
 564 constrained variational framework. In *International conference on learning representations*, 2017.

565

566 Dieuwke Hupkes, Verna Dankers, Mathijs Mul, and Elia Bruni. Compositionality decomposed:
 567 How do neural networks generalise? *Journal of Artificial Intelligence Research*, 67:757–795,
 568 2020.

569

570 Aaron Hurst, Adam Lerer, Adam P Goucher, Adam Perelman, Aditya Ramesh, Aidan Clark, AJ Os-
 571 trow, Akila Welihinda, Alan Hayes, Alec Radford, et al. Gpt-4o system card. *arXiv preprint
 572 arXiv:2410.21276*, 2024.

573

574 Takuya Ito, Murray Campbell, Lior Horesh, Tim Klinger, and Parikshit Ram. Quantifying artificial
 575 intelligence through algebraic generalization. *arXiv preprint arXiv:2411.05943*, 2024.

576

577 Aaron Jaech, Adam Kalai, Adam Lerer, Adam Richardson, Ahmed El-Kishky, Aiden Low, Alec
 578 Helyar, Aleksander Madry, Alex Beutel, Alex Carney, et al. Openai o1 system card. *arXiv
 579 preprint arXiv:2412.16720*, 2024.

580

581 Albert Qiaochu Jiang, Alexandre Sablayrolles, Arthur Mensch, Chris Bamford, Devendra Singh
 582 Chaplot, Diego de Las Casas, Florian Bressand, Gianna Lengyel, Guillaume Lample, Lucile
 583 Saulnier, Lélio Renard Lavaud, Marie-Anne Lachaux, Pierre Stock, Teven Le Scao,
 584 Thibaut Lavril, Thomas Wang, Timothée Lacroix, and William El Sayed. Mistral 7b. *ArXiv*,
 585 abs/2310.06825, 2023. URL <https://api.semanticscholar.org/CorpusID:263830494>.

586

587 Jared Kaplan, Sam McCandlish, Tom Henighan, Tom B Brown, Benjamin Chess, Rewon Child,
 588 Scott Gray, Alec Radford, Jeffrey Wu, and Dario Amodei. Scaling laws for neural language
 589 models. *arXiv preprint arXiv:2001.08361*, 2020.

590

591 Brenden Lake and Marco Baroni. Generalization without systematicity: On the compositional skills
 592 of sequence-to-sequence recurrent networks. In *International conference on machine learning*,
 593 pp. 2873–2882. PMLR, 2018.

594

595 Brenden M Lake and Marco Baroni. Human-like systematic generalization through a meta-learning
 596 neural network. *Nature*, 623(7985):115–121, 2023.

597

598 Margaret Li, Sneha Kudugunta, and Luke Zettlemoyer. (mis) fitting: A survey of scaling laws. *arXiv
 599 preprint arXiv:2502.18969*, 2025.

594 Aixin Liu, Bei Feng, Bing Xue, Bingxuan Wang, Bochao Wu, Chengda Lu, Chenggang Zhao,
 595 Chengqi Deng, Chenyu Zhang, Chong Ruan, et al. Deepseek-v3 technical report. *arXiv preprint*
 596 *arXiv:2412.19437*, 2024.

597

598 Brando Miranda, Alycia Lee, Sudharsan Sundar, Allison Casasola, and Sanmi Koyejo. Beyond
 599 scale: The diversity coefficient as a data quality metric for variability in natural language data.
 600 *arXiv preprint arXiv:2306.13840*, 2023.

601 Sarthak Mittal, Sharath Chandra Ruparthi, Irina Rish, Yoshua Bengio, and Guillaume Lajoie. Com-
 602 positional attention: Disentangling search and retrieval. *arXiv preprint arXiv:2110.09419*, 2021.

603

604 Mehryar Mohri, Afshin Rostamizadeh, and Ameet Talwalkar. *Foundations of machine learning*.
 605 MIT press, 2018.

606 Niklas Muennighoff, Alexander Rush, Boaz Barak, Teven Le Scao, Nouamane Tazi, Aleksandra
 607 Piktus, Sampo Pyysalo, Thomas Wolf, and Colin A Raffel. Scaling data-constrained language
 608 models. *Advances in Neural Information Processing Systems*, 36:50358–50376, 2023.

609

610 Maya Okawa, Ekdeep S Lubana, Robert Dick, and Hidenori Tanaka. Compositional abilities emerge
 611 multiplicatively: Exploring diffusion models on a synthetic task. *Advances in Neural Information
 612 Processing Systems*, 36:50173–50195, 2023.

613 Core Francisco Park, Maya Okawa, Andrew Lee, Ekdeep S Lubana, and Hidenori Tanaka. Emer-
 614 gence of hidden capabilities: Exploring learning dynamics in concept space. *Advances in Neural
 615 Information Processing Systems*, 37:84698–84729, 2024.

616 David Patterson, Joseph Gonzalez, Quoc Le, Chen Liang, Lluis-Miquel Munguia, Daniel Rothchild,
 617 David So, Maud Texier, and Jeff Dean. Carbon emissions and large neural network training. *arXiv
 618 preprint arXiv:2104.10350*, 2021.

619

620 Amir Rahimi, Vanessa D’Amario, Moyuru Yamada, Kentaro Takemoto, Tomotake Sasaki, and
 621 Xavier Boix. D3: Data diversity design for systematic generalization in visual question answer-
 622 ing. *arXiv preprint arXiv:2309.08798*, 2023.

623 Rahul Ramesh, Ekdeep Singh Lubana, Mikail Khona, Robert P Dick, and Hidenori Tanaka. Com-
 624 positional capabilities of autoregressive transformers: A study on synthetic, interpretable tasks.
 625 *arXiv preprint arXiv:2311.12997*, 2023.

626 John E Savage. *Models of computation*, volume 136. Addison-Wesley Reading, MA, 1998.

627

628 Shai Shalev-Shwartz and Shai Ben-David. *Understanding machine learning: From theory to algo-
 629 rithms*. Cambridge university press, 2014.

630

631 Paul Soulos, Edward J Hu, Kate McCurdy, Yunmo Chen, Roland Fernandez, Paul Smolensky, and
 632 Jianfeng Gao. Differentiable tree operations promote compositional generalization. In *Inter-
 633 national Conference on Machine Learning*, pp. 32499–32520. PMLR, 2023.

634

635 Paul Soulos, Henry Conklin, Mattia Opper, Paul Smolensky, Jianfeng Gao, and Roland Fernan-
 636 dez. Compositional generalization across distributional shifts with sparse tree operations. *arXiv
 637 preprint arXiv:2412.14076*, 2024.

638

639 Petru Soviany, Radu Tudor Ionescu, Paolo Rota, and Nicu Sebe. Curriculum learning: A survey.
International Journal of Computer Vision, 130(6):1526–1565, 2022.

640

641 Emma Strubell, Ananya Ganesh, and Andrew McCallum. Energy and policy considerations for
 642 modern deep learning research. In *Proceedings of the AAAI conference on artificial intelligence*,
 643 volume 34, pp. 13693–13696, 2020.

644

645 Arnas Uselis, Andrea Dittadi, and Seong Joon Oh. Does data scaling lead to visual compositional
 646 generalization? *arXiv preprint arXiv:2507.07102*, 2025.

647

648 Ashish Vaswani, Noam Shazeer, Niki Parmar, Jakob Uszkoreit, Llion Jones, Aidan N Gomez,
 649 Łukasz Kaiser, and Illia Polosukhin. Attention is all you need. *Advances in neural informa-
 650 tion processing systems*, 30, 2017.

648 Pablo Villalobos, Anson Ho, Jaime Sevilla, Tamay Besiroglu, Lennart Heim, and Marius Hobbhahn.
 649 Will we run out of data? limits of llm scaling based on human-generated data. *arXiv preprint*
 650 *arXiv:2211.04325*, 2022.

651

652 Benjie Wang, Denis Mauá, Guy Van den Broeck, and YooJung Choi. A compositional atlas for alge-
 653 braic circuits. *Advances in Neural Information Processing Systems*, 37:141318–141355, 2024a.

654

655 Xin Wang, Hong Chen, Si’ao Tang, Zihao Wu, and Wenwu Zhu. Disentangled representation learn-
 656 ing. *IEEE Transactions on Pattern Analysis and Machine Intelligence*, 46(12):9677–9696, 2024b.

657

658 Yaohui Wang, Xinyuan Chen, Xin Ma, Shangchen Zhou, Ziqi Huang, Yi Wang, Ceyuan Yang, Yinan
 659 He, Jiashuo Yu, Peiqing Yang, et al. Lavie: High-quality video generation with cascaded latent
 660 diffusion models. *International Journal of Computer Vision*, 133(5):3059–3078, 2025.

661

662 Jason Wei, Xuezhi Wang, Dale Schuurmans, Maarten Bosma, Fei Xia, Ed Chi, Quoc V Le, Denny
 663 Zhou, et al. Chain-of-thought prompting elicits reasoning in large language models. *Advances in*
 664 *neural information processing systems*, 35:24824–24837, 2022.

665

666 Thaddäus Wiedemer, Prasanna Mayilvahanan, Matthias Bethge, and Wieland Brendel. Composi-
 667 tional generalization from first principles. *Advances in Neural Information Processing Systems*,
 668 36:6941–6960, 2023.

669

670 Mengzhou Xia, Sadhika Malladi, Suchin Gururangan, Sanjeev Arora, and Danqi Chen. Less: Se-
 671 lecting influential data for targeted instruction tuning. *arXiv preprint arXiv:2402.04333*, 2024.

672

673 Sang Michael Xie, Shibani Santurkar, Tengyu Ma, and Percy S Liang. Data selection for language
 674 models via importance resampling. *Advances in Neural Information Processing Systems*, 36:
 675 34201–34227, 2023.

676

677 Yongyi Yang, Core Francisco Park, Ekdeep Singh Lubana, Maya Okawa, Wei Hu, and Hidenori
 678 Tanaka. Swing-by dynamics in concept learning and compositional generalization. *arXiv preprint*
 679 *arXiv:2410.08309*, 2024.

680

681 Zichun Yu, Spandan Das, and Chenyan Xiong. Mates: Model-aware data selection for efficient
 682 pretraining with data influence models. *Advances in Neural Information Processing Systems*, 37:
 683 108735–108759, 2024.

684

685 Chi Zhang, Huaping Zhong, Kuan Zhang, Chengliang Chai, Rui Wang, Xinlin Zhuang, Tianyi Bai,
 686 Jiantao Qiu, Lei Cao, Ju Fan, et al. Harnessing diversity for important data selection in pretraining
 687 large language models. *arXiv preprint arXiv:2409.16986*, 2024.

688

689 Dora Zhao, Jerone TA Andrews, Orestis Papakyriakopoulos, and Alice Xiang. Position: measure
 690 dataset diversity, don’t just claim it. *arXiv preprint arXiv:2407.08188*, 2024.

691

692

693 Xiang Zhou, Yichen Jiang, and Mohit Bansal. Data factors for better compositional generalization.
 694 *arXiv preprint arXiv:2311.04420*, 2023.

695

696 Roland S Zimmermann, Yash Sharma, Steffen Schneider, Matthias Bethge, and Wieland Brendel.
 697 Contrastive learning inverts the data generating process. In *International conference on machine*
 698 *learning*, pp. 12979–12990. PMLR, 2021.

699

700

701

ACKNOWLEDGEMENT

The authors used large language models (LLMs) as tools to assist with polishing the writing of this manuscript. The use of LLMs was limited to improving clarity and readability; all technical content, ideas, analyses, and conclusions are work of the authors.

A LIMITATION

While our work offers a theoretical and empirical analysis of how data diversity affects model generalization, it has several limitations. First, our framework treats semantic diversity and structural diversity as independent factors, ignoring their potential interactions. In practice, such interactions likely exist and may influence the optimal balance between the two. Second, we do not explore alternative training strategies, such as explicitly decomposing problems into subproblems and training models on them or curriculum training (Soviany et al., 2022). Our analysis is restricted to settings where such decomposition is not feasible. Finally, we do not provide concrete methods to measure semantic diversity, structural diversity, component complexity, or compositional complexity. As a result, our contributions remain a high-level principles rather than operational metrics.

B RADEMACHER COMPLEXITY

Uniform convergence is a sufficient condition for learnability, and Rademacher complexity measures the rate of uniform convergence. We define a hypothesis class \mathcal{H} , loss function l , the set of all possible input-output pairs consistent with the same underlying compositional structure \mathbb{D}_c and the training dataset $\mathbb{D}'_c = \{(f_c(x_{c,m}), y_{c,m}) | m \in [M]\} \subset \mathbb{D}_c$. To simplify notation, define the function class:

$$\mathcal{G} := l \circ \mathcal{H}.$$

For any $g \in \mathcal{G}$ and corresponding $h \in \mathcal{H}$, define the generalization and empirical errors as:

$$\text{err}_{\mathbb{D}_c}(h) = \mathbb{E}_{\mathbb{D}_c}[g(f_c(\cdot), y_c)], \quad \text{err}_{\mathbb{D}'_c}(h) = \frac{1}{M} \sum_{m=1}^M g(f_c(x_{c,m}), y_{c,m}).$$

Let σ be a vector of independent and identically distribution (i.i.d.) Rademacher variable such that $P[\sigma_m = 1] = P[\sigma_m = -1] = 0.5$. The empirical Rademacher complexity of \mathcal{G} with respect to dataset \mathbb{D}' , is defined as follows:

$$\text{Rad}_{\mathbb{D}'_c}(\mathcal{G}) = \frac{1}{M} \mathbb{E}_{\sigma \sim \{\pm 1\}^M} [\sup_{g \in \mathcal{G}} \sum_{m=1}^M \sigma_m g(f_c(x_{c,m}), y_{c,m})].$$

More generally, given a set of vectors, $\mathcal{A} \subset \mathbb{R}^M$, the Rademacher complexity of \mathcal{A} is:

$$\text{Rad}(\mathcal{A}) = \frac{1}{M} \mathbb{E}_{\sigma \sim \{\pm 1\}^M} [\sup_{a \in \mathcal{A}} \sum_{m=1}^M \sigma_m a_m].$$

Assuming the loss function $l(\cdot)$ is bounded by a constant λ , for all $h \in \mathcal{H}$ we have:

$$\text{err}_{\mathbb{D}_c}(h) - \text{err}_{\mathbb{D}'_c}(h) \leq 2\text{Rad}_{\mathbb{D}'_c}(l \circ \mathcal{H}) + 4\lambda\sqrt{\frac{2\ln(4/\delta)}{M}},$$

with probability of at least $1 - \delta$. This is result in derived using standard uniform coverage arguments (Shalev-Shwartz & Ben-David, 2014).

C TRADE-OFF BETWEEN DATA EFFICIENCY AND GENERALIZATION ERROR

Assume that all possible combinations can be embedded in a d -dimensional space \mathcal{V} by an embedding function $\phi(\cdot)$, where each composition corresponds to a point in this space. The model \mathcal{M} is

756
757
758
759
760
761
762
763
764
765
766
767
768
769
770
771
772
773

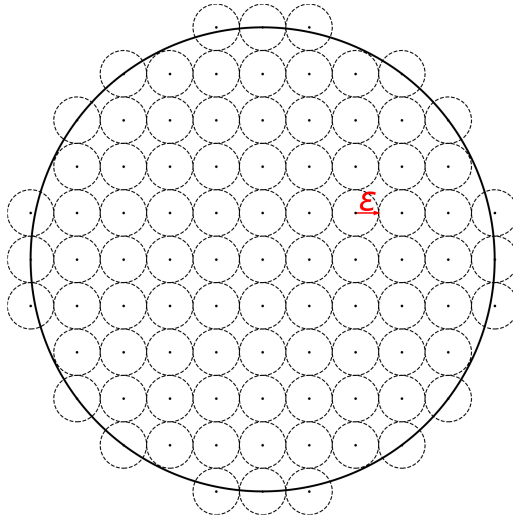


Figure 7: Covering a compositional space with ϵ -radius balls. Each point represents a composition observed in the training set, and the model is expected to generalize to nearby points. Increasing the number of training examples reduces the radius ϵ , yielding finer coverage of the space. Conversely, with fewer training examples, each ball must have larger radius to cover the space, leading to higher generalization error.

778
779
780

781 expected to generalize to similar compositions, i.e., nearby points in the d -dimensional space. As
782 shown in Figure 7, the model can generalize to points with distance at most ϵ centered at each training
783 composition with acceptable error. For example, if the training composition corresponds to the
784 circuit $c_1(\cdot) = ((x + y) + z) \cdot w$, then a structurally nearby variant such as $c_2(\cdot) = (x + (y + z)) \cdot w$
785 falls in the ϵ -radius ball (i.e., $|\phi(c_1) - \phi(c_2)| \leq \epsilon$). In contrast, a structurally far variant such as
786 $c_3(\cdot) = (x + y) \cdot (z + w)$ would lie outside the ϵ -radius ball (i.e., $|\phi(c_1) - \phi(c_3)| > \epsilon$).

787 Generalization, in this view, corresponds to covering the entire conceptual space from the sampled
788 compositions, where the radius ϵ reflects the upper bound of generalization error. When the training
789 dataset contains only a few compositions, covering the whole space requires each ball to have a
790 larger radius (i.e., larger ϵ), which implies higher generalization error. In contrast, when the training
791 set includes more diverse compositions, the space can be covered more densely using many smaller
792 balls, each with a smaller radius (i.e., smaller ϵ), leading to lower generalization error.

793

794

795 D CHAIN-OF-THOUGHT OF SOLVING ALGEBRAIC CIRCUIT

796

797

798 Below is an example of the CoT format used to fine-tune LLMs on the algebraic circuit tasks.

799

800 Example 1: CoT Example

801

802 **Question:** $4 \times (5 \times 2 + 5)$

803

804 **CoT:** We solve this step by step:

805 1. $4 \times (10 + 5)$

806 2. 4×15

807 3. 60

808 4. 60 Mod 10, the final answer is 0.

809

810
811
812 Table 1: Hyperparameters of the one-layer transformer model used in our experiments.
813
814
815
816

Layer	Output Size	Details
Input Embedding	32	Token embedding + positional encoding
Transformer Block	32	One-layer transformer block
Attention heads	32	16 attention heads

817
818
819 Table 2: Training hyperparameters for the encoder-only classification model.
820
821
822
823
824
825
826

Parameter	Value
Batch size	128
Learning rate	1×10^{-3}
Weight decay	0.01
Max sequence length	256
Number of epochs	100

830
831 D.1 ENCODER-ONLY MODEL
832
833
834

We use a single layer encoder-only transformer as the classification model. The architecture and training hyperparameters are summarized in Table 1 and Table 2, respectively.

835
836 E GENERATE GSM-STYLE EXAMPLES
837
838

We use GPT-4o to generate GSM-style questions and answers, including the question, CoT reasoning, and final answer. To ensure the generated examples follow the same reasoning path as seed examples from GSM8K, we use a prompt that preserves the logical structure while altering the surface realization (e.g., names, numbers, and context). The prompt used is shown below:

Example 2: Prompt
<p>You are given a GSM problem and its full solution. Your task is to generate a similar question:</p> <ol style="list-style-type: none"> 1. Has a different surface realization (different names, quantities, etc.). 2. Has a correct answer. 3. Requires the same reasoning process as the original one. 4. Produces a full GSM-style answer: <ul style="list-style-type: none"> - Includes reasoning steps - Give the final answer using the format: ### answer <p>Original Problem: {original question} Original Answer: {original answer} Now write the question and answer pair please: Output: Question: ... Answer: ...</p>

859
860 An example pair of GSM8K seed example and the generated example is provided:
861
862
863

864
865**Example 3: Pair of example**

866

Seed Example:

867

Question: Natalia sold clips to 48 of her friends in April, and then she sold half as many clips in May. How many clips did Natalia sell altogether in April and May?

870

Answer: Natalia sold $48/2 = << 48/2 = 24 >> 24$ clips in May. Natalia sold $48 + 24 = << 48 + 24 = 72 >> 72$ clips altogether in April and May. ### 72

873

Generated Example:

874

Question: Daniel baked 48 cookies in the morning, and then he baked twice as many cookies in the afternoon. How many cookies did Daniel bake altogether in the morning and afternoon?

878

Answer: Daniel baked $48 \times 2 = << 48 * 2 = 96 >> 96$ cookies in the afternoon. Daniel baked $48 + 96 = << 48 + 96 = 144 >> 144$ cookies altogether in the morning and afternoon. ### 144

882

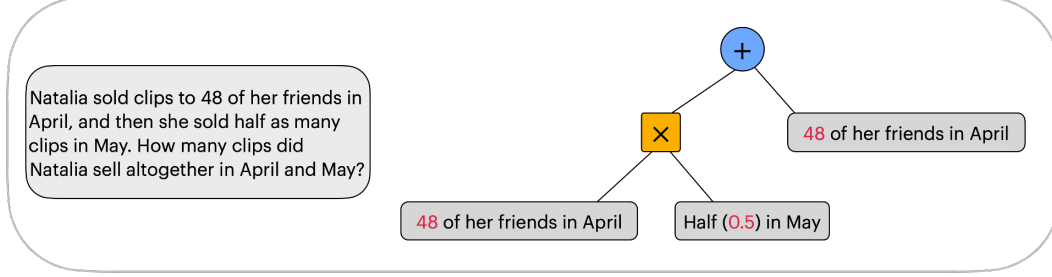
883

F GSM PROBLEM AS CIRCUIT

885

Mathematical problems can be naturally abstracted into circuit structures and by decomposing them into functional components, as shown in Figure 8. For example, the problem in GSM8K “*Natalia sold clips to 48 of her friends in April, and then she sold half as many clips in May. How many clips did Natalia sell altogether in April and May?*” can be decomposed into computing the number of clips sold in May and summing the totals from April and May. Each component corresponds to a node in the circuit, and the entire problem forms a compositional structure analogous to an algebraic circuit.

892



893

894

895

Figure 8: Decomposition of a GSM8K problem with circuit. The problem is represented as a composition of functional nodes: one computes May sales $48 \times 0.5 = 24$, and another combines April and May sales via $48 + 24 = 72$ to yield the final answer.

900

901

902

903

904

905

906

907

908

G SYNTHETIC SETUP

909

910

911

912

913

914

915

916

917

In the synthetic algebraic circuit dataset, each circuit corresponds to an algebraic expression such as $4 \times (5 \times 2 + 5)$. By computing the result modulo 10, the problem becomes a modular arithmetic, where the model needs to predict the output value between 0 and 9. We enforce the dataset to be balanced across classes, since otherwise results equal to 0 would dominate disproportionately. We further introduce variability through sub-circuits, where a full circuit can be composed of smaller sub-circuits as shown in Figure 9, which illustrated how sub-circuits are reused across compositions. We ensure that circuits in both the training and testing sets to be constructed from the same set of components. Increasing the depth of sub-circuits raises the component complexity. By adjusting circuit structure, sub-circuit depth, number of distinct structures (N), and number of realizations

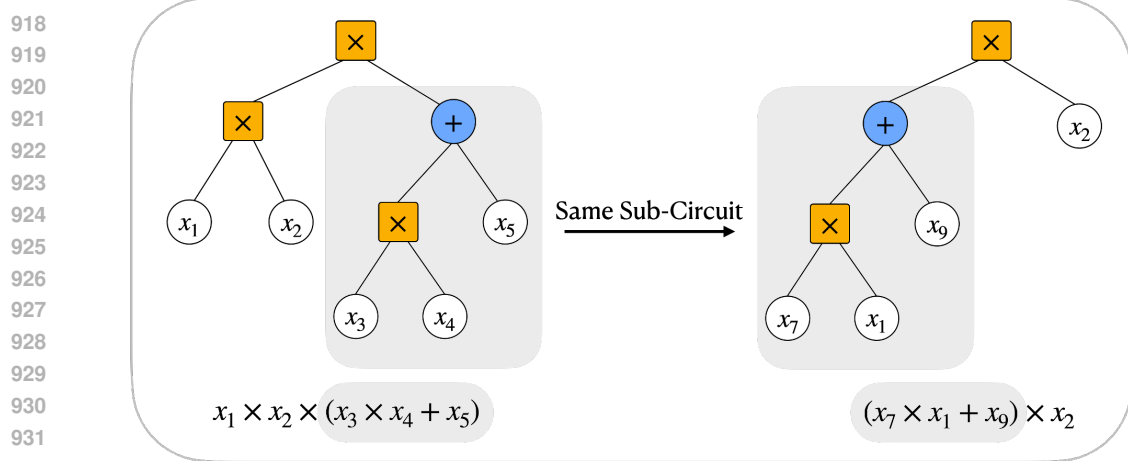


Figure 9: Example of basic component sharing in algebraic circuits. Each full circuit is composed of sub-circuits (components), which may be reused across different compositions. The depth of a sub-circuit determines the component complexity, while the way components are combined controls the overall structural diversity.

of the same underlying structure (M), we can systematically vary both semantic and structural diversity, as well as the component and structural complexity. We construct the dataset under a fixed budget of K training examples. Specifically, we select N distinct circuit structures, and generate M surface realizations for each structure, ensuring $K = M \cdot N$. In this way, structural diversity is determined by N , while semantic diversity is determined by M .

938
939
940
941
942
943
944
945
946
947
948
949
950
951
952
953
954
955
956
957
958
959
960
961
962
963
964
965
966
967
968
969
970
971